



Finite element analysis of fluid–structure interaction for the design of MAV aerodynamic shape



Y. Yu ^{a,b,c,*}, Q. Yang ^b, X. Wang ^{a,c}

^a State Key Laboratory of Precision Measurement Technology and Instruments, Tianjin University, Tianjin 300072, China

^b School of Engineering and Design, Brunel University, London UB8 3PH, UK

^c MOEMS Education Ministry Key Laboratory, Tianjin University, Tianjin 300072, China

ARTICLE INFO

Article history:

Received 10 October 2011

Received in revised form 4 January 2013

Accepted 30 January 2013

Available online 16 February 2013

Keywords:

Fluid–structure interaction

Finite element analysis

Micro air vehicle

Aerodynamic shape

Aerodynamic characteristic

ABSTRACT

In the study of micro aircraft flexible aerodynamic shape, the flexible structure interface deforms due to the air pressure, and this deformation simultaneously in turn affects the flow distribution around it, which is called a fluid–structure interaction problem. This paper discusses the general approach to such a fluid–structure interaction and further presents a detailed comparison between two representative materials used as aircraft surfaces. Two structure surfaces are respectively composed of natural rubber with high elasticity and steel alloy 1020 with high stiffness. In the test environment, the experimental model has a velocity of 8 m/s relative to the airflow, and the Reynolds number is higher than 5.44×10^4 . The simulations of the two aerodynamic models using the two materials were performed in ANSYS CFX. The simulation results have shown that the aerodynamic shape with flexible rubber material has greater deformation and smaller force peak amplitude than the rigid material aerodynamic shape, which is a good factor to maintain flight stability. It is concluded that the flexible material with higher flexibility and shock-absorbing capability used as micro aircraft shape can play a buffer role especially in the aerodynamic disturbance.

© 2013 Elsevier Ltd. All rights reserved.

1. Introduction

Micro Air Vehicles (MAVs) have begun to play an important role in recent years in many fields, both military and civilian. But due to MAVs' small size, light weight, low speed and fast response, external disturbances become more pronounced. With the rapid development of MAVs, the demands for flight stability and anti-gust disturbance ability have increased. Better designs of unique aerodynamic shape and various materials have been gradually adopted in the process of research. In order to improve the adaptive performance of aircrafts, aeroelastic analysis can be performed during the development of vehicles design [1], another approach is to study the effects of flight dynamics and nonlinear aeroelasticity of the flexible aircraft [2], and flexible materials with deformable aeroelastic property have been used on the aircraft configuration structures. The main reason for using this flexible material as the aircraft surface is that this kind of material has a damping effect and shock absorbing capacity which could improve the flight stability and anti-gust disturbance ability.

This research concerns a fluid–structure interaction issue, a type of multi-field analysis research. Multi-field research is actually an interdisciplinary finite element analysis, which focuses on the information transmission among different fields. Other common coupled-field problems include Joule heating within electric or structural coupling, electric machines within magneto or structural coupling, MEMS actuation within electrostatic or structural coupling, induction heating within harmonic electromagnetic or thermal coupling and so on.

Fluid–structure interaction (FSI) is one of the main areas in interdisciplinary finite element analysis, which is composed of finite element structural analysis and finite element fluid analysis. Such fluid–structure interaction problems appear frequently in practice, for example hydraulic shock absorbers, sloshing problem [3] and biomedical flow in flexible pipes. A systematic computational study of the hypersonic aeroelastic and aerothermoelastic behavior of a three-dimensional configuration was presented in the Ref. [4]. In this reference McNamara et al. developed an aerothermoelastic methodology that incorporates the heat transfer between the fluid and structure based on computational-fluid-dynamics-generated aerodynamic heating. Kalro et al. [5] presented a parallel finite element computational approach for 3D simulation of FSI in parachute system. They used a parallel computation within a message-passing programming environment to

* Corresponding author at: State Key Laboratory of Precision Measurement Technology and Instruments, Tianjin University, Tianjin 300072, China. Tel.: +86 13752430545.

E-mail address: jesuisynn@hotmail.com (Y. Yu).

Nomenclature

ρ_1	density of natural rubber, kg/m ³	ρ	average density of fluid, kg/m ³
E_1	Young's Modulus of natural rubber, GPa	γ	kinematic viscosity of fluid, m ² /s
ν_1	Poisson coefficient of natural rubber	μ	dynamic viscosity of fluid, kg/m s
ρ_2	density of steel alloy 1020, kg/m ³	U	mean velocity of the object relative to the fluid, m/s
E_2	Young's Modulus of steel alloy 1020, GPa	H	height of the micro air vehicle, mm
ν_2	Poisson coefficient of steel alloy 1020	R	external radius of the shell structure, mm
T	temperature of two-dimensional incompressible viscous Newton flow, °C	r	internal radius of the cylindrical vertical duct, mm
		t	thickness of the shell, mm

implement flow and structure dynamics solvers. Zhang et al. [6] employed arbitrary Lagrangian–Eulerian (ALE) finite element formulation and adopted a strong coupling strategy with some stabilization techniques for fluid–structure interaction such as the simulation of the pulsation of a 2D artificial heart pump and a 3D simplified model with structural buckling. Nomura et al. developed a computational method for a class of fluid–structure interaction problems [7] and then added a procedure to express free surface motion [8]. This computational method is shown through vortex-induced vibration of a circular cylinder as well as TLD–structure interaction problem (Tuned liquid damper is designed to suppress a particular single vibration mode of the objective structure). Sun et al. [9] used multi-field ALE method to analyze fluid–structure interaction dynamics on water impact of projectile. The results showed the pressure applied from fluid on projectile as well as projectile attitude and position variation, which can be used to determine appropriate initial attitude in water impact of projectile. Fluid–structure interaction problems usually occur in aircraft such as wing vibration. Dubcova et al. [10] researched the interaction between turbulent flow and a vibrating airfoil, and simulated the pressure distribution as well as the flow dynamics. For the moving flexible foil, Shin et al. [11] developed a new method in fluid–structure interaction analysis. The simulation results showed that moving flexible foil can generate much larger vertical force than the corresponding rigid one.

In the whole system consisting of vehicle and air flow, the fluid pressure at the interface can be applied as a load on the structure and the resulting displacement as well as the velocity obtained could be passed on as a load to the fluid, which is actually a bi-directional fluid–structure interaction problem. This coupling interaction between flexible structure and flow fluid around takes place in space–time phase, especially when the mesh deformation of the fluid area is obvious or the geometrical configuration of structure is complicated.

Fluid–structure interaction problems and multi-field problems in practice are complex and it is necessary to study them with experiments as well as numerical simulations. Gomes et al. [12] presented a comparison between numerical and experimental results for a two-dimensional, self-excited periodic motion of an elastic, free vibrating structure, and have achieved good agreement between their results. It is essential to validate the fluid–structure interaction analysis based on comparison with experimental data.

The rest of this paper is organized as follows. Section 2 addresses the content and significance of the research about MAV flexible aerodynamic shape as a fluid–structure interaction problem. Section 3 briefly summaries the computation and simulation method of computational fluid dynamics in relation to fluid–structure interaction problem. The ANSYS multi-field solver technology has been implemented in this study. Section 4 compares two kinds of materials' multi-field simulation results. Section 5 discusses and concludes the paper.

2. Definition of test case

2.1. MAV structure and air flow definition

The choice of aircraft materials significantly affects its flight performance. Due to the specific application demand, hyperelastic material is recently used for the aerodynamic shape of aircraft. In particular, natural rubber has been widely applied in the fields of aerospace and manufacturing with its high flexibility and shock absorbing capacity. The volume of rubber remains constant during its deformation process and this deformation is a recoverable deformation. In addition, the incompressible characteristic of natural rubber is very close to the ideal material ($E = 0.5$). As an aircraft shape material, steel alloy 1020 with high stiffness is considered in the comparative simulation. Steel alloy 1020 is a kind of Plain Low-Carbon Steel, which is typically used in structural and pipe applications. The mechanical properties and values of natural rubber and metal steel, a reference material usually used in aircraft structure, are listed in Table 1.

Two-dimensional incompressible viscous Newtonian flow is simulated in this paper. The state of the fluid is listed in Table 2. The mean velocity of the object relative to the fluid is $U = 8$ m/s.

Vertical take-off and landing and hover capabilities are the primary characteristics of hovering MAV. The hovering MAV model designed in this article consists of lifting system, vertical duct and aerodynamic shape. The aerodynamic shape is a symmetrical structure and its structural geometry is shown in Fig. 1 and the parameters are listed in Table 3. In order to observe the variations including the airflow distribution around the MAV and the aero-elastic deformations produced on its surface under airflow pressure, an observation point is set on the windward of the model. The figure also shows an airflow of 8 m/s in X direction, relative to the coordinate system given in the figure.

2.2. Fluid–structure interaction problem

Usually there are two types of fluid–structure interaction problems, one-way FSI and two-way FSI. In the two-way fluid–structure interaction problem, the flow pressure causes the structure surface to deform and move which in turn alters the fluid pressure

Table 1
Mechanical properties of two materials.

Mechanical properties	Materials	
	Natural rubber ^a	Steel alloy 1020 ^b
Density/kg m ⁻³	$\rho_1 = 913$	$\rho_2 = 7850$
Young's Modulus/GPa	$E_1 = 0.02$	$E_2 = 207$
Poisson coefficient	$\nu_1 = 0.49$	$\nu_2 = 0.30$

^a Data from www.Wikipedia.com.

^b Data from [13].

Table 2
Properties of the simulated fluid.

$T/^\circ\text{C}$	15
$\rho/\text{kg m}^{-3}$	1.225
$\gamma/\text{m}^2 \text{s}^{-1}$	$14.7\text{e}-6$
$\mu/\text{kg m}^{-1} \text{s}^{-1}$	$1.8\text{e}-5$

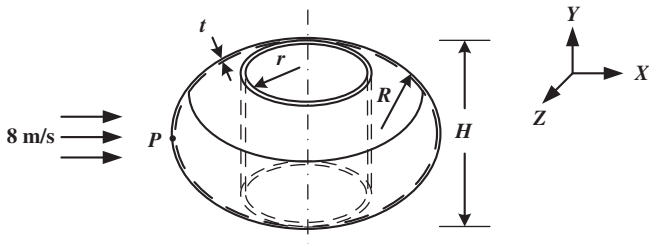


Fig. 1. Structural geometry of the hovering MAV.

Table 3
Geometrical parameters.

H/mm	100
R/mm	50
r/mm	50
t/mm	2

distribution around and the dynamic force on the structure. During the fluid–structure interaction, this coupling phenomenon is usually significant as shown in Fig. 2. Since this interaction is transient, the pressure on the structure surface and the displacement at the fluid–structure interface are continuous. It is necessary to couple the fluid physics and structural physics at each time step throughout the computation, rather than just by transferring data from one domain to the other at the end of the simulation. Therefore, in this article, the structure domain is calculated by ANSYS and the fluid domain is computed by CFX, both results are transferred at each time step of simulation using unsteady aeroelastic Euler Navier–Stokes solving equation.

3. Computation and simulation

3.1. Arbitrary Lagrangian–Eulerian method

Lagrangian description and Eulerian description of motion usually apply in the continuum mechanics analysis [14]. Lagrangian method is widely used in structure mechanics, which is easy to track free surface and interface between different materials. Each individual node of the computational mesh attaches to material particle during motion. On the other hand, Eulerian method is mainly used in fluid dynamics. The nodes of computational mesh

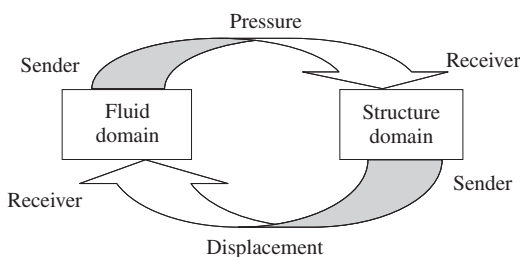


Fig. 2. Structure–fluid interaction.

are fixed in one space and independent to material particle. So the arbitrary Lagrangian–Eulerian (ALE) finite element simulation is an approach to combine the advantages of two classical kinematical descriptions while avoiding some disadvantages that the traditional Lagrangian finite element simulation and Eulerian finite element simulation have. When using the ALE algorithm, the nodes of the mesh can move along with material particles in Lagrangian manner or be fixed in the space in Eulerian manner, or move arbitrarily to optimize the element shapes and rezone continuously. This method is appropriate for modeling the fluid domain and solving fluid–structure interaction problems. A schematic diagram of ALE method is shown in Fig. 3.

In the diagram, the Ω^F is the spatial fluid domain with boundary Γ^F , consisting of fluid material particles. Here, Γ^F is not the end of fluid domain but is a boundary between computational fluid domain and Euler fluid. Ω^S is the spatial structure domain made up of structural material particles and $\Omega^{S'}$ is the spatial structure domain after its movement. Γ^{FS} is the structure boundary interfacing with the fluid domain. Across Γ^{FS} interface the coupling is enforced by transferring the displacement from the structure to the fluid domain, and in turn the surface pressure from the fluid to structure domain. In addition, u is the velocity of fluid material and u' is the velocity of moving mesh from the spatial domain Ω . The relative velocity between the material and the mesh from the spatial domain is defined as $c = u - u'$.

According to the above ALE method, the Lagrangian description is applied on the structure as well as its moving boundary Γ^{FS} and every node of mesh follows the associated material points. So the mesh velocity coincides with the material velocity, $u' = u$ and the velocity c is null. In the meantime Eulerian description is employed far away from the moving boundary, in the ideal Euler fluid as well as Γ^F . Each node of computational mesh is fixed in the space, $u' = 0$ and the velocity c is identical to the material velocity u . A transition region is defined in between and described by ALE method. The mesh in this computational domain could be moved arbitrarily according to the material point to optimize the element shapes and keep continuity. The ALE approach in the coupling mesh generally performs better to follow large distortions and offers higher resolution to track free surface of structure.

3.2. Mesh control method

When the structure moves or deforms, the finite element computational mesh over the fluid domain will deform in accordance with the free surface motion. If the shape of structure is simple and deformation of the body is negligible in comparison with its deflection, the fluid domain does not need to re-mesh. If the shape of structure is complex or it has significant deformation on the interface, the transition fluid domain needs to re-mesh and update. And the re-mesh method strongly affects the performance of the ALE technique.

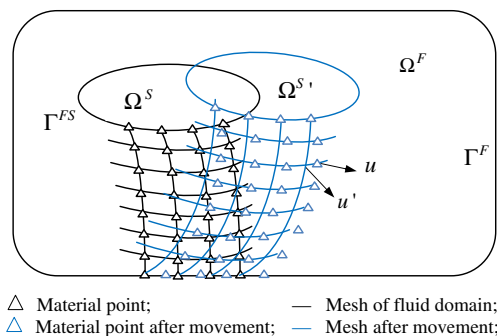


Fig. 3. Schematic diagram of ALE method.

At the interface of fluid and structure domain, the relationship of two meshes usually exists either matching or non-matching. In an ideal situation, the coupling between fluid and structure requires that one fluid node and one solid node are placed at the same point at the interface to ensure the velocities or displacements coincide along the interface and could be transferred freely. But the actual situation is that two computational meshes of fluid and structure domain might be generated independently and the coupled data needs to be transferred across two dissimilar meshes. Therefore, necessary interpolation methods are required to implement load transferring task.

3.3. ANSYS multi-field solver technology

In this investigation, ANSYS multi-field solver technology is applied to implement the object model, the coupling algorithm, the mesh updating, the data computation and the final results. Multi-field solver provides a convenient framework to solve coupled field problems. For the fluid–structure interaction problem, the structural part of the analysis is solved using the ANSYS solver and the fluid part using the CFX solver. Moreover, the multi-filed solver technology allows the structure and fluid solutions to run in parallel and transfer data simultaneously.

Usually, the mesh of fluid domain is more refined than the structure mesh. Two interpolation algorithms are usually used in the ANSYS multi-field solver to transfer coupled data across two dissimilar meshes, one is profile preserving interpolation and the other is globally conservative interpolation.

In the process of displacement transferring from structure to fluid domain, the profile preserving interpolation is used between sender and receiver as shown in Fig. 4. Each node R_i on the receiver side maps to an element s_i on the sender side and s_i is the interpolation data from its two adjacent node data (S_i). So the transferring process is sending displacement from the interpolation elements s_i on the structure domain to nodes R_i on the fluid domain.

Globally conservative interpolation is used in the process of pressure transferring from fluid to structure domain, as shown in Fig. 5. Unlike the profile preserving interpolation method, each node S_i on the sender side divides the pressure data of fluid domain into two parts and transfers them to the nearest element nodes R_i on the receiver side. The cumulative transfer variables on the nodes R_i are the received data on structure surface.

4. Results and comparison

In order to investigate that different materials have different effects in the fluid–structure interaction process, two kinds of representative materials are adopted as model surface material for such problem. It is well known that natural rubber has high elasticity and flexibility, and usually plays the role of buffer in some vibration system. On the contrary, rigid steel alloy has high stiffness and less capability of elastic deformation. Both of these two materials have certain representativeness. In the simulation, however, the aircraft geometries and environmental parameters are set the

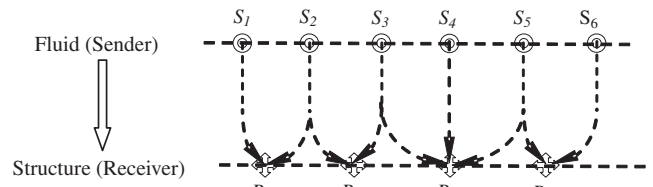
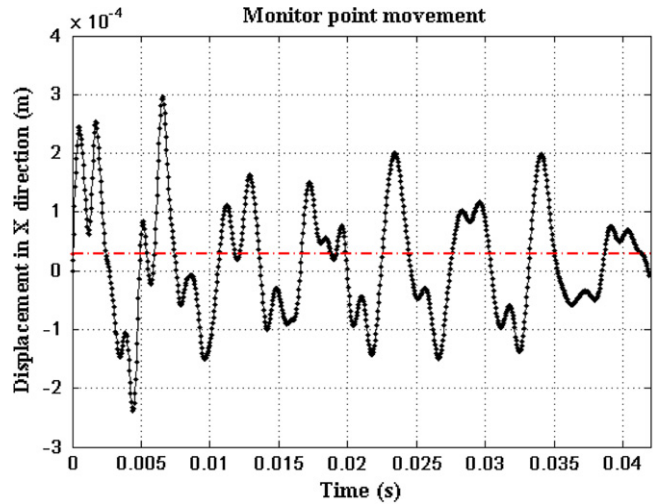
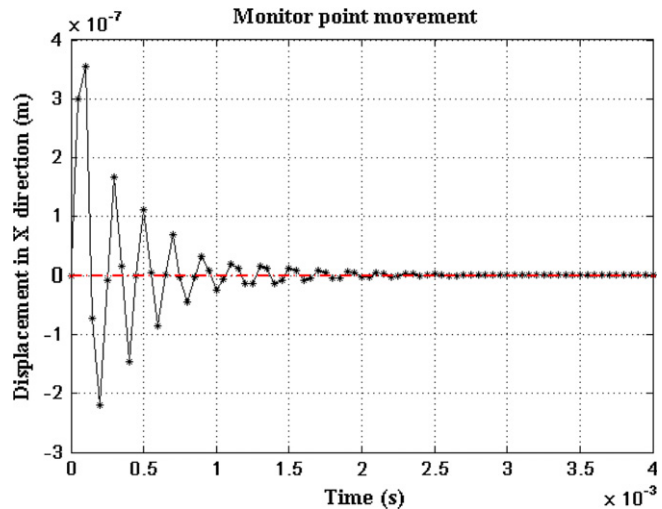


Fig. 5. Globally conservative interpolation.



(a) Flexible rubber



(b) Rigid steel alloy

Fig. 6. Monitor point displacement in X direction.

same. The calculation step time is set 0.05 ms and the velocity of the input disturbance flow imitates an 8 m/s constant speed in X direction.

4.1. Deformation of aircraft shape

In order to observe the deformation of the aerodynamic shape caused by fluid pressure, a monitor point is located at the top of interface which is the initial action position in fluid–structure interaction. Under the same situation, due to the air pressure, two model shapes with different materials will produce a force

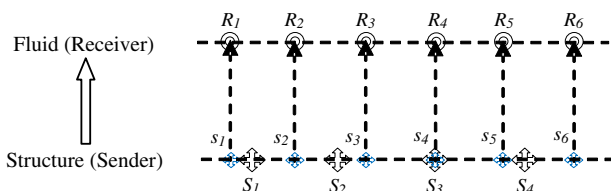


Fig. 4. Profile preserving interpolation.

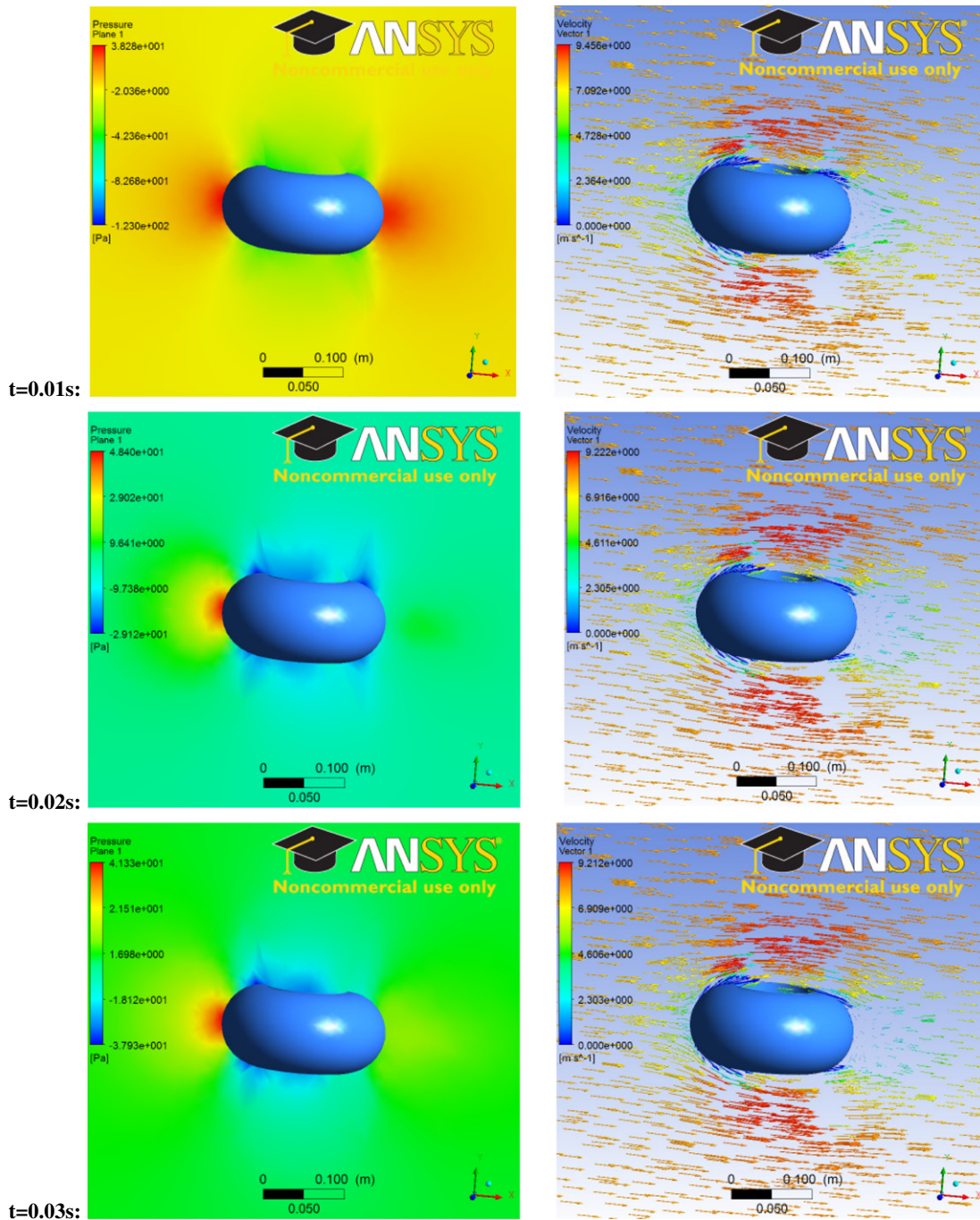


Fig. 7. The distribution of the pressure (left) and the velocity vector (right) of aerodynamic shape with flexible rubber material at different instant.

vibration respectively. Moreover, some transient vibrations are superimposed on the first few peaks. The displacement of the monitor point in X direction is shown in Fig. 6.

The results in Fig. 6 showed that the flexible rubber material has resulted in significant higher vibration amplitude than the rigid steel alloy material. The maximum vibration amplitude on the flexible surface is 0.3 mm, but the rigid surface has peak amplitude less than 0.4 μm . Due to the high elasticity of the flexible interface, the force vibration will last a longer time, which is more than 0.04 s, compared with only about 2.5 ms for the steel alloy material. In addition, due to its high stiffness, the rigid material appears to recover to its original geometrical shape after vibration despite the sustained flow pressure. In Fig. 6, the final recovery state of the

aerodynamic shape is represented by the red¹ dot-dashed line. On the other hand, the structure made of flexible rubber material will maintain a certain amount of deformation on the structure surface, which remains in the stable state.

4.2. Distribution of the pressure and velocity fields

In order to understand the aerodynamic characteristics of considered materials and models, in particular, the effect of the

¹ For interpretation of color in Fig. 6, the reader is referred to the web version of this article.

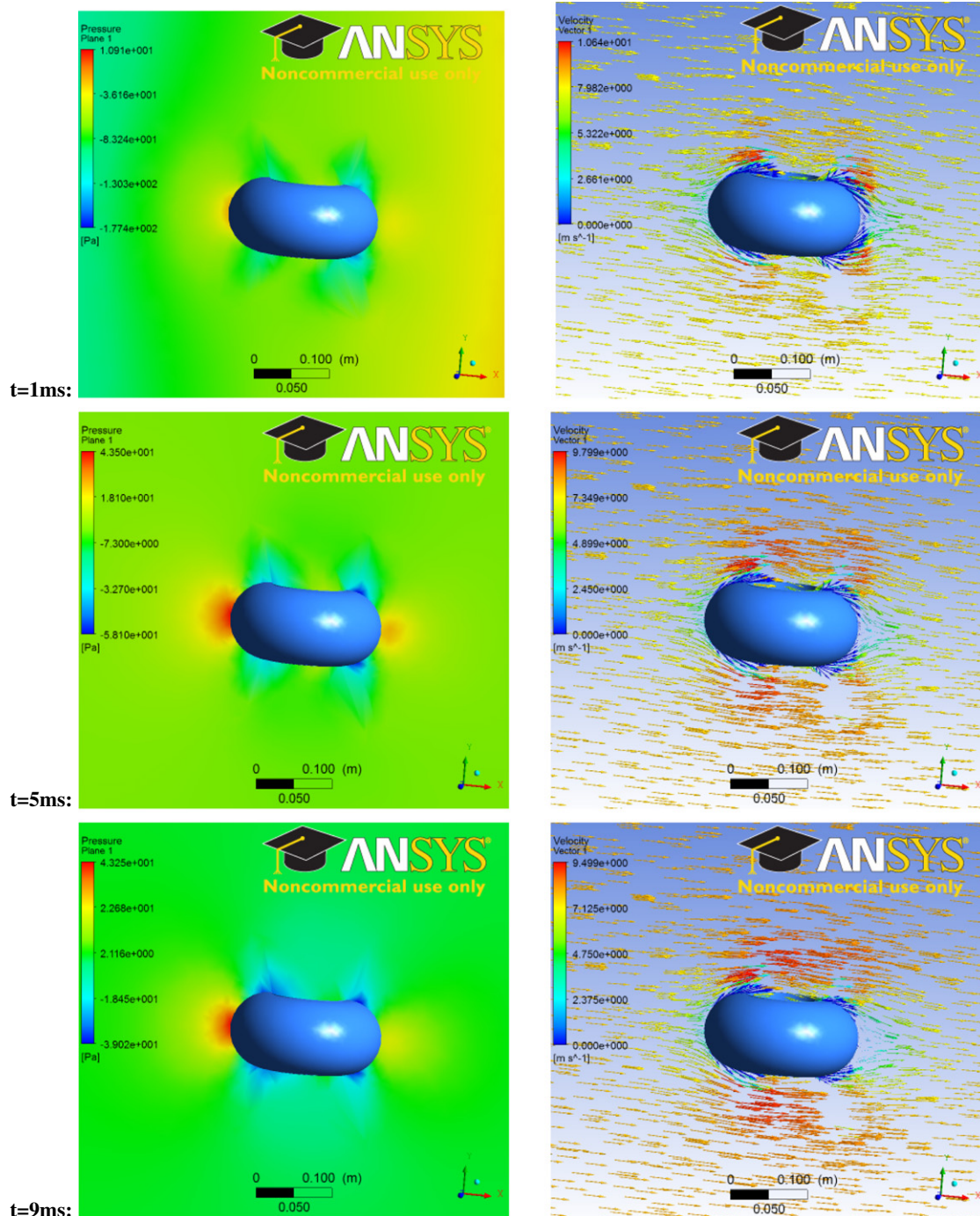


Fig. 8. The distribution of the pressure (left) and the velocity vector (right) of aerodynamic shape with rigid steel alloy material at different instants.

vibration on flight stability, it is useful to examine the detailed pressure and velocity fields. Figs. 7 and 8 represented the dynamic pressure distributions (left) and velocity vector distributions (right) on the symmetry plane of aircraft aerodynamic models with different materials at different instants.

Figs. 7 and 8 showed that the pressure value around the observation point P gradually become larger and then smaller. For instance, in Fig. 7, the pressure value of P is approximate 38.2 Pa at the first observation time, 48.4 Pa at the second observation time and then 41.3 Pa at the third observation time. In Fig. 8, the pressure value of P is approximate 10.9 Pa at the first observation time, 43.5 Pa at the second observation time and then 43.2 Pa at the third observation time. Such transient change

appears to be produced by the interaction between the fluid and structure. This interaction could significantly affect the dynamic deformation of the front surface on the aircraft model, and the transient change of air pressure will usually cause the force in X direction to change during a short time. In addition, the velocity vector plots indicated that the airflow velocity above and below the model appears to increase. According to the Bernoulli's principle, there is an inversely proportional relationship between the pressure and the velocity. For example, the air pressure above the model decreases as the flow velocity increases. Since the lift on the aircraft model results from the air pressure difference above and below, the lift will vary constantly as time goes on.

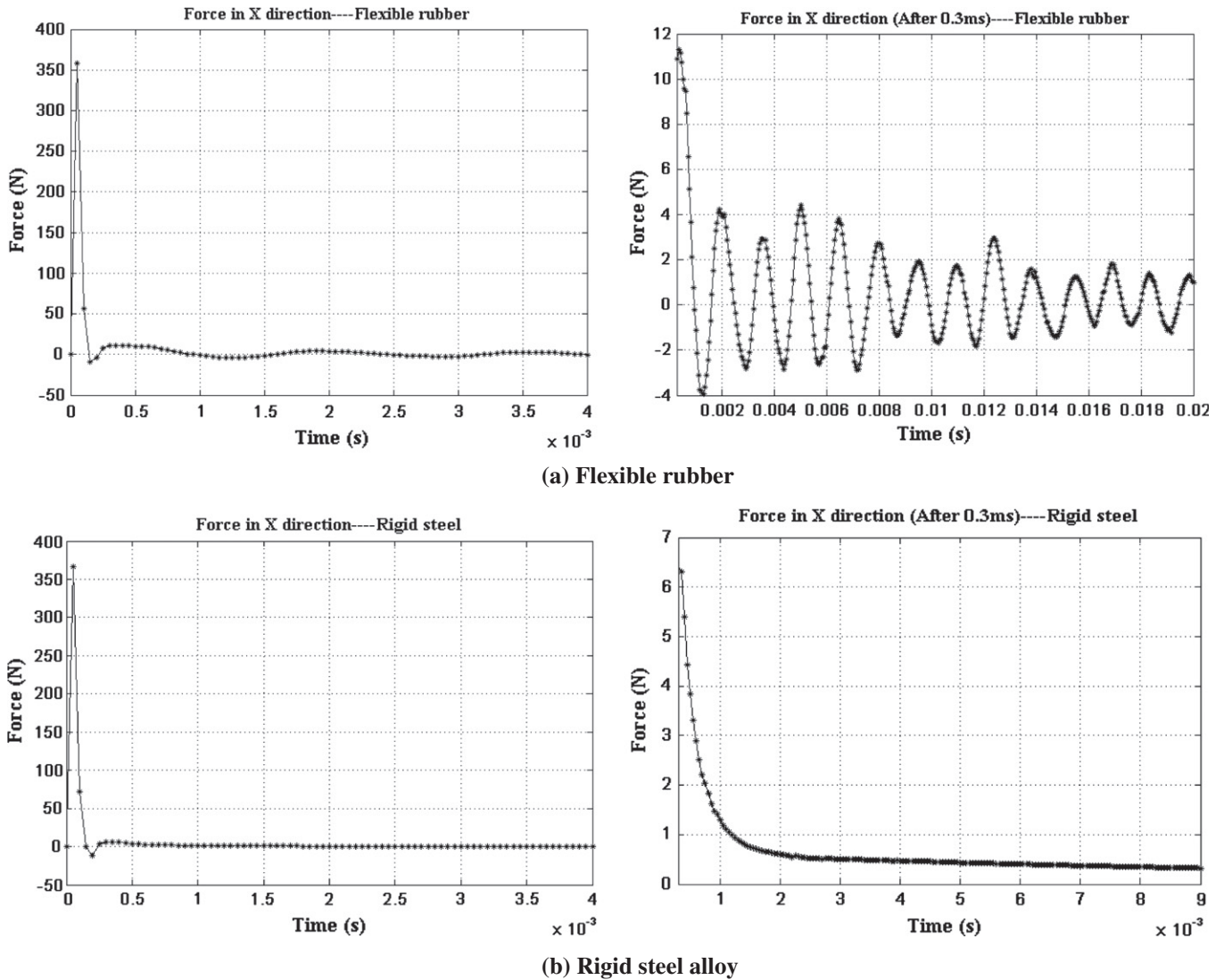


Fig. 9. Force in X direction.

4.3. Forces at the interface

The forces generated on the flexible material aerodynamic shape and the rigid material one in X direction can be seen in Fig. 9. For each material, the left side plots show the initial responses, whilst the right side plots detail the responses some time later (i.e. after 0.3 ms). The forces generated in Y direction are presented in Fig. 10.

In Fig. 9, the force amplitude produced by the rigid material model appears almost the same as the flexible material model in the flow velocity direction. In flight, the force in X direction is a considerable influence in terms of model postural stability and flight balance. Usually, this air disturbance should be reduced as much as possible by optimizing the geometrical parameters and mechanical properties of the structure during the aircraft design process. After 0.3 ms, the flexible material model appears to be in a state of thrust and drag balance condition but the rigid material model remains in the thrust from the beginning to end. There is a significant difference in maintaining flight stability. To some extent, it illustrates that the aerodynamic shape made of flexible rubber material could adjust the balance during the flight and has a good shock absorbing capacity in the gust. The flexible aerodynamic shape will recover the stable state from vibration after a

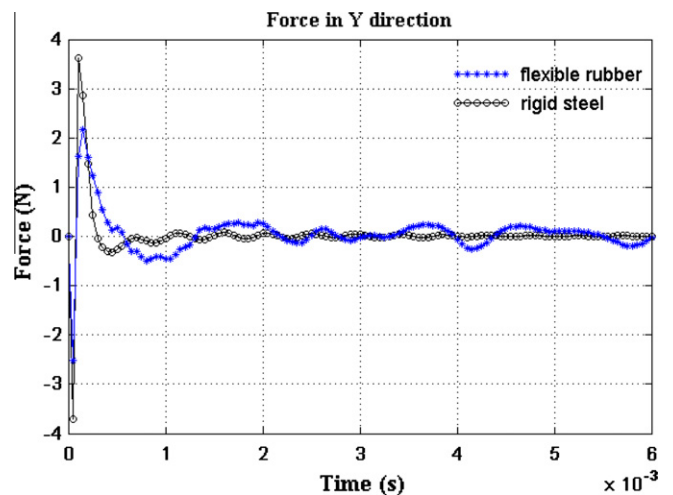


Fig. 10. Force in Y direction.

relative longer time compared with the rigid surface. During a long period of vibration, the flexible material may absorb the disturbance force on the aircraft and thus keep the flight more stable.

In Fig. 10, the initial force generated on the rigid material shape in Y direction is larger compared with flexible material model. Usually, the force response in Y direction and rapid change are considerable disadvantageous impact for aircraft stability in flight. Here the force generated on the flexible material shape in this direction is slightly smaller, which produces little effect during the aircraft flight and performs better anti-disturbance capability. Similarly, the flexible aerodynamic shape has a longer settling time than the rigid one.

5. Conclusions

A numerical study of MAV flexible aerodynamic shape has been reported as a fluid–structure interaction problem. In the micro aircraft design process, more flexible materials have been adopted as structure surface for improving flight stability and enhancing anti-disturbance capability. In this paper, some information about fluid–structure interaction issue is introduced, especially for the MAV aerodynamic shape in the flight. Under the airflow disturbance or wind gust, the structure surface deforms due to the flow pressure, in turn this deformation changes the distribution of fluid domain around it. This is a dynamic interaction process which happens all the time during the flight.

Based on the hovering MAV aerodynamic shape, finite element analysis and simulation using ANSYS multi-field solver technology have been performed to verify how the interactions affect the aerodynamic characteristics. In the simulation, two representative materials are adopted as the aircraft structural surfaces, one is flexible rubber material with high elasticity and the other rigid steel alloy material with high stiffness. Both of them have the same geometrical dimensions and environmental conditions. The comparisons show that: (a) the flexible rubber material with higher flexibility and elasticity has greater deformation than rigid steel alloy and the displacement vibration lasts a longer time; (b) compared with the rigid material, the force generated in Y direction seems to have smaller peak amplitudes, which is a good advantage in maintaining flight stability. We can conclude that due to the greater vibration and deformation on the flexible material shape, the aerodynamic characteristic has good potential to improve aircraft flight stability and to enhance anti-disturbance capability as

well. The research on fluid–structure interaction can help designer to complete the design and optimization of aircraft aerodynamic shape and to improve the flight performance.

Acknowledgements

This work was financially supported by Support Program of National Ministry of Education of China (No. 625010110), National Natural Science Foundation of China (No. 61179043), and Specialized Research Fund for the Doctoral Program (SRFDP) of Higher Education (No. 20070056085).

References

- [1] Bhatia KG. Airplane aeroelasticity: practice and potential. *J Aircraft* 2003;40(6):1010–8.
- [2] Zhao ZJ, Ren GX. Multibody dynamic approach of flight dynamics and nonlinear aeroelasticity of flexible aircraft. *AIAA J* 2011;49(1):41–54.
- [3] Mitra S, Sinhamahapatra KP. 2D simulation of fluid–structure interaction using finite element method. *Finite Elem Anal Des* 2008;45(1):52–9.
- [4] McNamara JJ, Friedmann PP, Powell KG, Thuruthimattam BJ. Aeroelastic and aerothermoelastic behavior in hypersonic flow. *AIAA J* 2008;46(10):2591–610.
- [5] Kalro V, Tezduyar TE. A parallel 3D computational method for fluid–structure interactions in parachute system. *Comput Method Appl Mech Eng* 2000;190(3–4):321–32.
- [6] Zhang Q, Hisada T. Analysis of fluid–structure interaction problems with structural buckling and large domain changes by ALE finite element method. *Comput Method Appl Mech Eng* 2001;190(48):6341–57.
- [7] Nomura T, Hughes TJR. An arbitrary Lagrangian–Eulerian finite element method for interaction of fluid and rigid body. *Comput Method Appl Mech Eng* 1992;95(1):115–38.
- [8] Nomura T. ALE finite element computations of fluid–structure interaction problems. *Comput Method Appl Mech Eng* 1994;112(1–4):291–308.
- [9] Sun Q, Zhou J, Lin P. Dynamic analysis of fluid–structure interaction for water impact of projectile using LS-DYNA. *J Syst Simul* 2010;22(6):1498–501.
- [10] Dubcova L, Feistauer M, Horacek J, Svacek P. Numerical simulation of interaction between turbulent flow and a vibrating airfoil. *Comput Vis Sci* 2009;12(5):207–25.
- [11] Shin S, Kim HT. Numerical simulation of fluid–structure interaction of a moving flexible foil. *J Mech Sci Technol* 2008;22(12):2542–53.
- [12] Gomes JP, Yigit S, Lienhart H, Schafer M. Experimental and numerical study on a laminar fluid–structure interaction reference test case. *J Fluid Struct* 2011;27(1):43–61.
- [13] Callister William Jr D. *Materials science and engineering: an introduction*. 6th ed. New York, Chichester: Wiley; 2003. p. 737–45.
- [14] Malvern LE. *Introduction to the mechanics of a continuous medium*. Englewood Cliffs: Prentice-Hall; 1969.